Founded 1905

APPLICATION OF ITERATIVE FEEDBACK TUNING

BY

DENG JIEWEN (B.S)
DEPARTMENT OF ELECTRICAL AND COMPUTER ENGINEERING

A THESIS SUBMITTED
FOR THE DEGREE OF MASTER OF ENGINEERING

NATIONAL UNIVERSITY OF SINGAPORE
2003

Acknowledgments

I would like to express my deepest gratitude to all those who have guided me for my postgraduate study in the National University of Singapore and Singapore Institute of Manufacturing Technology. First, I'd like to express my utmost gratitude to my supervisor, Associate Professor Ho Weng Khuen and Assistant Professor Tay Ee Beng for their guidance through my Master's study. Their unwavering confidence and patience have aided me tremendously. I have benefited a lot from their wealth of knowledge and accurate foresight.

Second, special thanks should be given to Associate Professor Ling Keck Voon in Nanyang Technological University, Singapore for his advice and support during my attachment in Singapore Institute of Manufacturing Technology. Indeed I benefited a lot from the discussions with Professor Ling. His knowledge and understanding on control impressed me very much.

Third, I would like to extend my special thanks to Dr. Chen Xiaoqi, Mr. Chow Siew Loong and Mr. Lok Boon Keng of Singapore Institute of Manufacturing Technology for their help and suggestions, especially on the VLSI process technology during my attachment there. Also, special thanks go to Mr. Hong Yang in University of Ottawa, Canada as well as many others in the Advanced Control Technology Lab in NUS. I enjoyed very much the time spent with them. I also appreciate the National University of Singapore for the research facilities and scholarship.

Finally, I would like to thank my family and friends for their support and understanding.

DENG, JIEWEN

May, 2003

Contents

Acknowledgements **i**

Summary **iv**

List of Tables **v**

List of Figures **vii**

1 Introduction **1**

1.1 Motivation 1

1.2 Contributions 4

1.3 Organization of the Thesis 5

2 Thickness uniformity control using Iterative Feedback Tuning **6**

2.1 Introduction 6

2.2 Experimental Setup 8

2.3 Resist Thickness Estimation 10

2.4 Iterative Feedback Tuning Control 13

2.5 Experimental results 16

2.6 Conclusions 22

3 Relay auto-tuning of PID controllers using Iterative Feedback Tuning **23**

3.1 Introduction 23

3.2 Iterative Feedback Tuning 24

3.3 Relay Auto-Tuning 26
3.4 The Proposed Algorithm 29
3.5 Choices of Phase Margin and Bandwidth 31
3.6 Examples 33
3.7 Conclusions 38

4 Conclusions **40**

4.1 Main Findings 40
4.2 Suggestions for Further Work 41

Bibliography **42**

Author's Publications **48**

Summary

Lithography technology has been one of the key enablers and drivers for the semiconductor industry for the past several decades. Improvements in lithography are responsible for roughly half of the improvement in cost per function in integrated circuit(IC) technology. In this thesis, in-situ process monitoring and Iterative Feedback Tuning(IFT) are used to control the resist thickness uniformity across the wafer, as well as to improve the convergence time to a specified reference thickness. Using an array of in-situ thickness sensors to measure the thickness, and the IFT algorithm to update the PI(Proportional Integral) controller, a real-time control strategy is implemented to control the resist thickness during softbake. An average of 19 times improvement in the resist thickness uniformity is achieved and the time to convergence is reduced significantly.

Also, the thesis investigated the application of IFT to auto-tune a PID controller during the relay experiment to give specified phase margin and bandwidth. Good tuning performance according to the specified phase margin and bandwidth can be obtained and the limitation of the standard relay auto-tuning technique using a version of the Ziegler-Nichols formula can be eliminated.

List of Tables

2.1 Controller parameter, non-uniformity, and convergence time for Zone 1 18
2.2 Controller parameter, non-uniformity, and convergence time for Zone 2 18
2.3 Summary of experiments. The first experiment is conventional softbake and the following 3 iterations of experiments are performed using the IFT approach 21
2.4 Improvement on the thickness uniformity 21

List of Figures

1.1 Variations of CD with resist thickness 3

2.1 The microlithography sequence. 7
2.2 Schematic of experimental setup to control the thickness in real-time. The system consists of a multi-zone bakeplate, thickness sensors and a computing unit. 9
2.3 Schematic of experiment setup to control the thickness, which consists of a multi-zone bakeplate, thickness sensors and a computing unit. . . 10
2.4 Thin film optical model 11
2.5 Variation of the reflectance signal with wavelength for a particular resist thickness 12
2.6 Conventional feedback system 14
2.7 Conventional softbake with bakeplate maintained at 90^oC: zone 1 and zone 2 are represented by dashed and dashed-dotted lines respectively. (a)Thickness, (b)Temperature, (c)Power. 17
2.8 3 iterations of Experiment A. (A-1) (A-4) (A-7) thickness, (A-2) (A-5) (A-8) temperature, (A-3) (A-6) (A-9) power. Two zones are monitored. Reference, zone 1 thickness measurement and zone 2 thickness measurement are represented by the solid, dashed and dashed-dotted lines respectively. 19

2.9 3 iterations of Experiment B. (B-1) (B-4) (B-7) thickness, (B-2) (B-5) (B-8) temperature, (B-3) (B-6) (B-9) power. Two zones are monitored. Reference for zone 1, reference for zone 2, zone 1 thickness measurement and zone 2 thickness measurement are represented by the solid, dotted, dashed and dashed-dotted lines respectively. 20

3.1 Conventional feedback system 25

3.2 Relay Tuning 27

3.3 Diagram for the relay auto-tuning experiment 34

3.4 Iterative Feedback Tuning. $P(s) = \frac{1}{(s+1)^6}$; y^d: dotted line; er: dashed line 34

3.5 Tuning result of Equation (3.29) 35

3.6 Ziegler-Nichols tuning 35

3.7 Coupled-tanks system 37

3.8 Real-time experimental result 38

Chapter 1

Introduction

1.1 Motivation

Input-output data-based controller design methods have been proposed by many researchers(Campi et al, 2002). These methods do not depend on the plant model, and utilize I/O data only. Among various I/O data-based design methods, one approach is the Iterative Feedback Tuning(IFT) scheme(Hjalmarsson et al, 1994). This scheme is based on iterative tuning of the controller parameters along the gradient direction of a given cost function, and is applicable when one stabilizing controller is given in advance. So far, many interesting results on IFT have been obtained. For instance, various IFT methods for nonlinear systems(Hjalmarsson, 1998) and MIMO systems(Hjalmarsson et al, 1998) have been developed. Also, tuning methods for various specifications such as settling time(Lequin et al, 1999) are discussed. Furthermore, evaluations of IFT with numerical simulations and experiments have been reported; for example, rolling mills(Hjalmarsson et al, 1999), robot joints(Gunnarsson et al, 1999) and thermal cycling modules(El-Awady et al, 1999).

In this thesis, ideas from IFT are incorporated into semiconductor manufacturing process control. With shrinking feature sizes, the challenge to maintain adequate and affordable process latitude becomes increasingly difficult. Advances in process control and metrology will be necessary to achieve less than 10 nm (3σ) gate critical dimension (CD) control, especially for 130 nm and below technology node(Marchetti,

1999). According to the International Technology Roadmap for Semiconductor in 1999, gate CD control of 10 nanometer is required at 100nm technology node by year 2005(International Technology Roadmap for Semiconductors: Lithography, 1999). The roadmap presents the industry-wide consensus on the R&D efforts needed to meet the challenges of semiconductor manufacturing at a specific minimum linewidth. By the year 2014, it is estimated that gate CD control of 4nm is required at the 35nm technology node. In addition to tightening process specifications, the industry is also moving towards 300 mm wafer for economic reasons. This places a stringent demand on all the lithographic processes as the control requirement is now stretched over a larger area. In additional, lithography on non-conventional substrates such as quartz photomask or LCD flat panel display manufacturing is also critical.

Due to thin film interference effects, CD varies with the resist thickness, as given in Figure 1.1. The resist thickness has to be well controlled to remain at the extrema of the swing curve where the sensitivity of CD to resist thickness variations is minimized. As the amplitude and periodicity of the swing curve increases with decreasing wavelength(Brunner, 1991), the control of the resist thickness and its uniformity across a larger substrate becomes increasingly important. Already for 200 mm substrate, resist thickness uniformity specification is met by having tight controls over important parameters such as relative humidity, temperature, spin speed, exhaust, etc. during spin coating (Levison, 1999). With a larger substrate, the specifications for these parameters are expected to be even more demanding, and the complexity of the coating process is expected to increase. The range of useful thickness for any fixed viscosity resist is also limited as the transition from laminar to turbulent flow now occurs at a lower spin speed. This transition to turbulent flow during spin coating is largely responsible for the increase in thickness non-uniformity at the edge of the wafer (A.B. Charles et al, 1999; E. Gurer et al, 2000). However, it is sometimes necessary to spin the resist at higher speed to obtain the optimum resist thickness, as indicated by the extrema of the swing curve.

Typical lithographic process begins with hexamethyldisilazane (HMDS) priming, followed by resist coating and then the softbake process. Softbake is an important

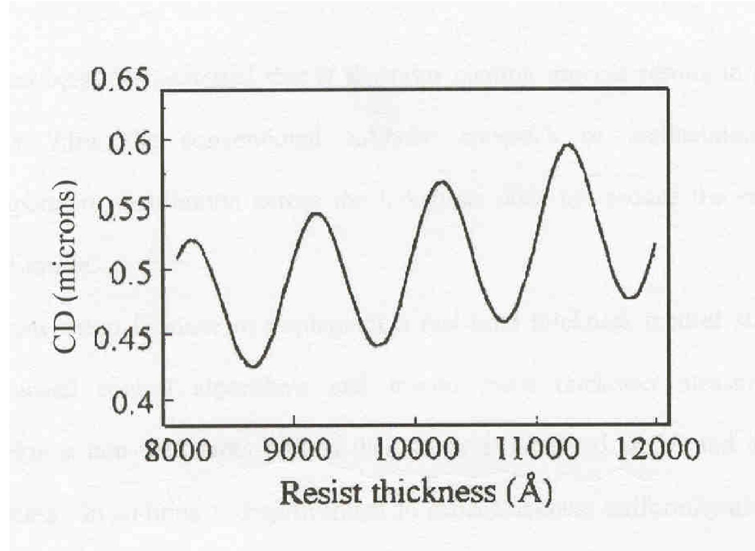

Figure 1.1. Variations of CD with resist thickness

process performed after coating the resist to remove excess solvent from the resist film, reduce standing waves and relax the resist polymer chain into an ordered matrix. As in all bake processes, temperature control (J. R. Sheats et al, 1998; Ho et al, 2000) during softbake is important. Conventionally, the resist is baked at a fixed temperature with temperature control of 1^oC for consistent lithographic performance. However, our experiment shows that maintaining a uniform temperature profile across the bakeplate does not reduce the resist film non-uniformity. In this thesis, we propose a model-free approach to improve resist thickness uniformity through the softbake process using Iterative Feedback Tuning(IFT).

Hjalmarsson et al. (1994, 1998) developed the theory of Iterative Feedback Tuning (IFT), a technique inspired by iterative identification and control schemes. It is entirely driven by closed-loop data obtained on the actual closed-loop system operating under a sequence of controllers. The iterative identification and control design scheme may be considered as a parameter optimization problem in which the optimization is carried directly on the controller parameters, thereby abandoning the need of identification of a model altogether. This property is especially helpful for thickness control, since it eliminates the need to get a precise model, and it's suitable for real application of different types of wafers with different properties.

However, the IFT in resist thickness control needs two experiments for each iteration in order to get the Input/Output data and compute the derivatives. In Chapter 3 of the thesis, we further investigate the application of IFT in the relay auto-tuning of PID controllers, which presents a model-based approach where the common modelling assumptions for relay systems in limit cycle are used. Based on these model assumptions for the relay system, the derivatives of the output with respect to the controller parameter can be derived analytically, thus eliminating the need of the second experiment in each iteration. The thesis investigates the application of IFT to relay auto-tuning of PID controller according to specified phase margin and bandwidth. It's addressed in detail in Chapter 3 of the thesis.

1.2 Contributions

The thesis has investigated and contributed to the following areas:

In Chapter 2, to implement thickness control during softbake, our approach uses an array of in-situ thickness sensors positioned above a multi-zone bakeplate to monitor the resist thickness. With these in-situ thickness measurements, the thickness profile of the photoresist is controlled in real-time by using the PI(Proportional Integral) controller, which is updated by the Iterative Feedback Tuning (IFT) control algorithm. It may be considered as a parameter optimization problem in which the optimization is carried directly on the controller parameters, thereby abandoning the need of identification of a model. The PI(Proportional-Integral) controller is tuned using IFT during the experiments to give good tuning performance. Thickness non-uniformity of less than 10nm at a specified target thickness may be achieved, with an average of 19$\times$ improvement in resist thickness uniformity at the end of the bake process. With the stringent demand of advanced lithography, this ability to squeeze out the last few nanometers of the process is important. This will also help to relax the tight specification of the coating process.

Chapter 3 investigates the application of IFT in relay auto-tuning of PID controllers. Good tuning performance according to the specified bandwidth and phase margin can be obtained and the limitation of the standard relay auto-tuning tech-

nique using a version of Ziegler-Nichols formula can be eliminated. In contrast, extra experiments are conducted to obtain these derivatives in the standard IFT algorithm because no such modelling assumptions are made.

1.3 Organization of the Thesis

The thesis is organized as follows. Chapter 2 focuses on the application of IFT to thickness uniformity control. Then in Chapter 3 ideas from IFT are incorporated into relay auto-tuning of PID controllers. Some simulation and implementation examples using IFT are given. Finally, conclusions and suggestions for further work are drawn in Chapter 4.

Chapter 2

Thickness uniformity control using Iterative Feedback Tuning

2.1 Introduction

With shrinking feature sizes and increasing wafer areas, it's increasingly difficult to achieve less than 10nm (3σ) gate critical dimension (CD) control. Due to thin film interference effects, CD varies with the resist thickness. The resist thickness has to be well controlled to remain at the extrema of the swing curve where the sensitivity of CD to resist thickness variations is minimized. Consider the lithography sequence which begins with a priming step to promote adhesion of polymer photoresist material to the substrate as shown in Figure 2.1. A thin layer of resist is then spin-coated on the surface. The solvent is evaporated from the resist by a baking process (softbake). Conventionally, the resist is baked at a fixed temperature with temperature control of 1^oC for consistent lithographic performance. However, our experiment shows that maintaining uniform temperature profile across the bakeplate does not reduce the resist film non-uniformity. In Palmer E. et al(1996), a run-to-run controller is used to control the photoresist thickness from wafer to wafer to a target thickness. We note that this is a "lumped" parameter approach in which only the mean photoresist thickness is controlled. In this chapter, we present another approach to improve wafer photoresist uniformity.

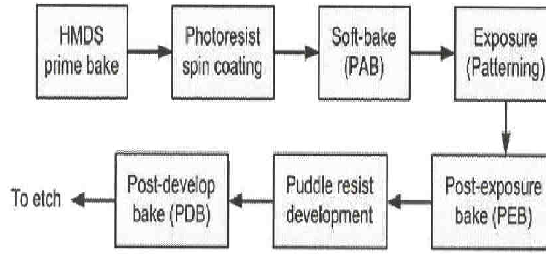

Figure 2.1. The microlithography sequence.

To implement thickness control during softbake, our approach uses an array of in-situ thickness sensors positioned above a multi-zone bakeplate to monitor the resist thickness. There has been some research on *in situ* monitoring of the resist thickness and properties during the bake process. To study the bake mechanism, Paniez et al. (P. J. Paniez et al, 1998) used *in-situ* ellipsometry while Fadda et al. (E. Fadda et al, 1996) used contact angle measurements to monitor the resist thickness during the bake process. Morton et al. (Morton S.L, 1999a; S. L. Morton et al , 1999b) used *in-situ* ultrasonic sensors to monitor the change in resist properties to determine whether the resist has been sufficiently cured, thereby determining the endpoint of the softbake process. In related work, Metz et al. (T. E. Metz et al, 1991) used *in-situ* multi-wavelength reflection interferometers to measure the resist thickness versus bake time to determine the optimum bake time.

With these *in-situ* thickness measurements, the thickness profile of the photoresist is controlled in real-time by manipulating the heater power distribution using advanced control algorithms. In Ho et al. (Ho et al, 2002) and Lee et al. (Lee L. L et al, 2002), a novel technique to control the resist thickness and improve its uniformity through the softbake process is proposed. In these previous approaches, the proposed control algorithms are model-based approaches: generalized predictive control (GPC) and sliding mode control. Identification of the system dynamics to generate the plant model is thus required for both approaches. This is usually time-consuming due to the need to obtain an adequate model of the system. In this chapter, we propose to tune the PI controllers using iterative feedback tuning algorithm (IFT). Hjalmarsson et. al. (Hjalmarsson et al, 1994, 1998) developed the theory of iterative feedback

tuning (IFT), a technique inspired by iterative identification and control schemes. It is entirely driven by closed-loop data obtained on the actual closed-loop system operating under a sequence of controllers. The iterative identification and control design scheme may be considered as a parameter optimization problem in which the optimization is carried directly on the controller parameters, thereby abandoning the step of identification of a model altogether. In general, this technique has the advantages of requiring no plant modelling, operating online while the system runs in closed loop, directly tuning the controller parameters along the gradient direction of a given cost function, and is applicable when one stabilizing controller is given in advance.

In this chapter, we not only use the *in-situ* thickness measurements to detect the endpoint of the softbake process but also improve the resist thickness uniformity by manipulating the bakeplate temperature distribution. Various zones on the wafer are made to follow a predefined thickness trajectory to reduce thickness non-uniformity at endpoint. The PI (Proportional-Integral) controller is tuned using IFT during the experiment to give good tuning performance. About 19$\times$ improvement of thickness uniformity is obtained. With the stringent demand of advanced lithography, this ability to squeeze out the last few nanometers of the process is important. This will also help to relax the tight specification of the coating process.

2.2 Experimental Setup

The experimental setup used to control resist thickness consists of three main parts (see Figure 2.2): a multi-zone bakeplate, thickness sensors and a computing unit. In all our experiments, thick film resist Clariant AZ4620 is spin-coated at 2000 rpm on a 4-inch wafer. Thickness at two zones, each 1 inch apart, are monitored and controlled to demonstrate the control strategy (see Figure 2.3). An array of 2 thickness sensors is mounted directly above the wafer at 2 zones where the resist film thickness are being controlled. Currently, the setup is for a 4-inch wafer (radius: 2 inches; 2 points monitored). This can be easily scaled to a 12-inch wafer (radius: 6 inches; 7 points monitored).

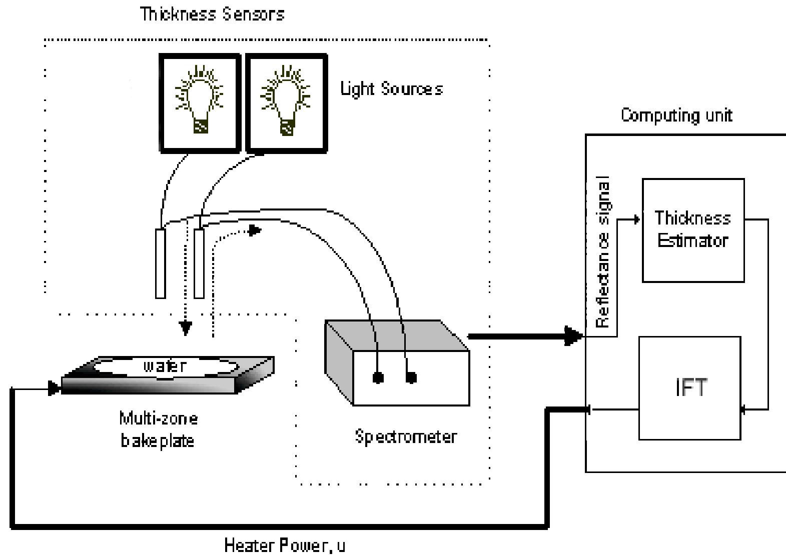

Figure 2.2. Schematic of experimental setup to control the thickness in real-time. The system consists of a multi-zone bakeplate, thickness sensors and a computing unit.

A. Multi-zone Bakeplate

Figure 2.3 shows the cross-section of the thermal processing module used. It consists of an array of independently controlled resistive heating elements with embedded resistance temperature detectors (RTDs). This gives us the flexibility to control thickness through temperature manipulation at different locations on the bakeplate. Small thermal mass and fast response time of the bakeplate make it suitable for our application. Depending on applications, the number of zones of the bakeplate can be easily configured. The details of the thermal processing module are published in (C.D. Schaper et al, 1999; El-Awady et al, 2000).

B. Thickness Sensor

The thickness sensor has a similar setup as the multi-wavelength DRM in Henderson(C.L. Henderson et al, 1998). It comprises a broadband light source (LS-1), a spectrometer with the capability of monitoring the reflected light intensity at three sites simultaneously (SQ2000) and a bifurcated fiber optics reflection probe (R200) from OceanOptics. The reflection probe consisting of a bundle of 7 optical fibers (6 illumination fibers around 1 read fiber) is positioned above the wafer to monitor the

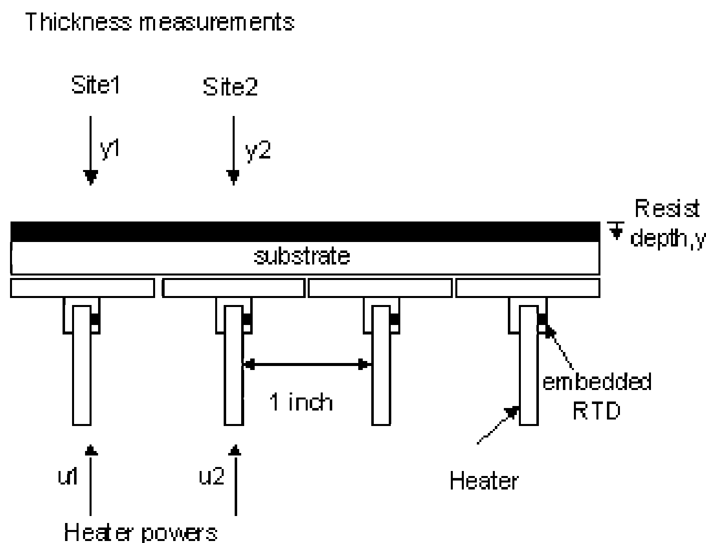

Figure 2.3. Schematic of experiment setup to control the thickness, which consists of a multi-zone bakeplate, thickness sensors and a computing unit.

resist thickness in real-time. During softbake, light from the broadband light source is focused on the resist through one end of the probe and the reflected light is guided back to the spectrometer through the other end.

C. Computing Unit

The resist thickness at various sites on the wafer are monitored by an array of thickness sensors. The reflectance signals are acquired through the A/D converter and the computing unit converts them to thickness measurements using a thickness estimation algorithm in Labview environment. The thickness estimation algorithm is discussed in Section 2.3. With the availability of the thickness measurements, the IFT algorithm updates the PI parameters to minimize resist thickness non-uniformity and reduce the time for convergence.

2.3 Resist Thickness Estimation

The thickness sensors, enclosed by the dotted lines in Figure 2.2, are used for in-situ measurements of the resist thickness, y. An optical model is used to estimate the resist

thickness from the reflectance signal, as shown in Figure 2.4. The model assumes normally incident light and homogenous resist film. During wafer processing, light from the broadband light source is focused normally onto the resist-coated wafer through illumination end of the bifurcated fiber optics reflection probe while the reflected light is guided back to the spectrometer through the read end of the reflection probe. Some of the incident light reflects at the top resist-ambient interface while part of the incident light propagates through the resist film and reflects at the substrate-resist interface. The additional optical path travelled creates a phase difference between the incident and reflected light. Constructive or destructive interference, which depends on the wavelength of the incident light and resist thickness, occurs in the resist film. Hence the reflectance signal, $h(\lambda, y)$, observed at the spectrometer also varies as a function of the resist thickness, y, and wavelength of the light source, λ (T.L. Vincent et al , 1997; Fowles G.R. et al, 1975). Figure 2.5 shows the typical variation of the reflectance signal with wavelength for a particular resist thickness.

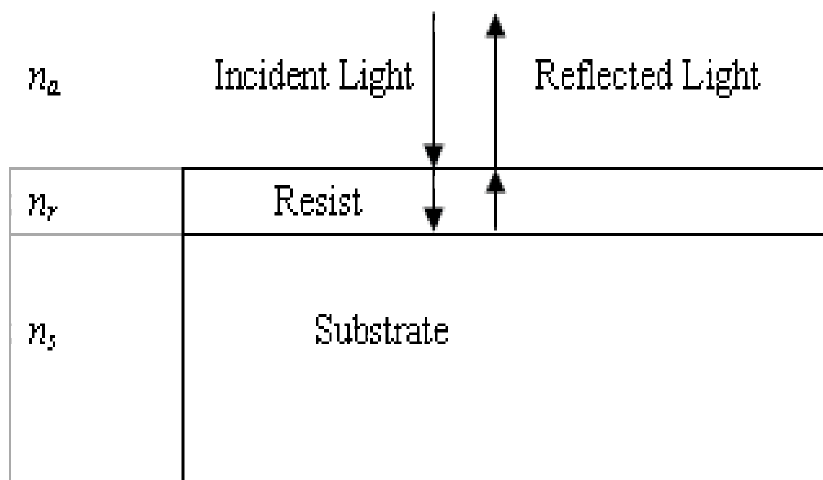

Figure 2.4. Thin film optical model

$$h(\lambda, y) = \left(\frac{r_2 e^{-i\delta} + r_1 e^{i\delta}}{r_1 r_2 e^{-i\delta} + e^{i\delta}} \right) \left(\frac{r_2 e^{-i\delta} + r_1 e^{i\delta}}{r_1 r_2 e^{-i\delta} + e^{i\delta}} \right)^* \tag{2.1}$$

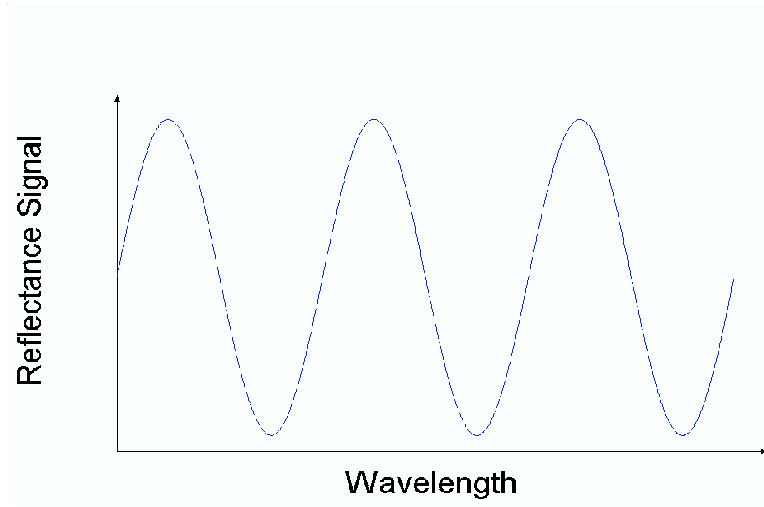

Figure 2.5. Variation of the reflectance signal with wavelength for a particular resist thickness

where

$$r_1 = \frac{n_a - n_r}{n_a + n_r} \qquad r_2 = \frac{n_r - n_s}{n_r + n_s} \qquad \delta = \frac{2\pi n_r y}{\lambda} \tag{2.2}$$

Also, na, nr and ns are the refractive index of air, resist and substrate respectively. The variation of the refractive index with wavelength, λ, is given by the Cauchy equation (Born M. et al, 1980):

$$n(\lambda) = A + \frac{B}{\lambda^2} + \frac{C}{\lambda^4} \tag{2.3}$$

where A, B and C are the Cauchy parameters of the resist such that $A = 1.6207$, $B = 2.91 \times 10^3 nm^2$ and $C = 2.78 \times 10^9 nm^4$ for the Clariant AZ4620 resist. In this study, we do not explicitly consider the effects of temperature on the Cauchy parameters over the bake processing window. This is separately investigated in (L.L. Lee et al, 2000).

Given the reflectance measurements, the resist film thickness may be estimated using Equation (2.1). However, we have a reasonably good initial estimate of the resist thickness from the coating process. Therefore, a local minimum solution for the

resist thickness is obtained using least squares estimation. To do this, Equation (2.1) is approximated by taking the Taylor series expansion such that

$$h(\lambda, y) = h(\lambda, y_0) + \frac{\partial h}{\partial y}|_{\lambda, y_0} \Delta y \tag{2.4}$$

where y_0 is the initial thickness estimate and $\frac{\partial h}{\partial y}$ the derivative. The estimated resist thickness $\hat{y}$ is given as

$$\hat{y} = y_0 + \Delta y \tag{2.5}$$

and the change in thickness, Δy, is estimated using the least squares estimation method given by

$$\Delta y = \left(\frac{\partial h}{\partial y}^T \frac{\partial h}{\partial y} \right)^{-1} \frac{\partial h}{\partial y}^T (h - h_0) \tag{2.6}$$

where

$$\frac{\partial h}{\partial y} = \begin{bmatrix} \frac{\partial h}{\partial y}|_{\lambda_1, y_0} \\ \frac{\partial h}{\partial y}|_{\lambda_2, y_0} \\ \vdots \\ \frac{\partial h}{\partial y}|_{\lambda_M, y_0} \end{bmatrix} \qquad h = \begin{bmatrix} h(\lambda_1, y) \\ h(\lambda_2, y) \\ \vdots \\ h(\lambda_M, y) \end{bmatrix} \qquad h_0 = \begin{bmatrix} h(\lambda_1, y_0) \\ h(\lambda_2, y_0) \\ \vdots \\ h(\lambda_M, y_0) \end{bmatrix} \tag{2.7}$$

To estimate the thickness, 1000 reflectance measurements (M = 1000) are obtained at wavelength between 450 nm and 800 nm, about 0.35 nm apart. A sampling period of 1 second is selected. The initial estimate, y_0, is updated with the current value at every sample.

2.4 Iterative Feedback Tuning Control

The IFT algorithm is described elsewhere in the literature (Hjalmarsson et al, 1994, 1998). In this section, only the equations necessary for our experiment is reviewed. Consider the conventional feedback system as shown in Figure 2.7:

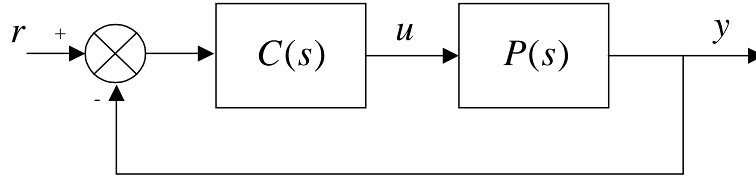

Figure 2.6. Conventional feedback system

A quadratic criterion is defined:

$$J(\rho) = \frac{1}{2N}\left[\sum_{t=1}^{N}(L_y\tilde{y}_t(\rho))^2 + \lambda\sum_{t=1}^{N}(L_u u_t(\rho))^2\right] \tag{2.8}$$

where ρ and N are the controller parameters and the number of data points considered respectively. The first term in Equation (2.8) is the frequency weighted (by a filter L_y) error between the desired response and the achieved response. The second term is the penalty on the control effort which is frequency weighted by a filter L_u. The filters L_y and L_u can be set to be 1, but they give added flexibility to the design. In the experiments, they are set to be 1. The user specified desired output is given as y_d and $\tilde{y}_t(\rho) = y_t(\rho) - y_d$.

To obtain the minimum of J we would like to find a solution for ρ to the equation

$$\frac{\partial J}{\partial \rho} = \frac{1}{N}\left[\sum_{t=1}^{N}\tilde{y}_t(\rho)\frac{\partial \tilde{y}_t}{\partial \rho}(\rho) + \lambda\sum_{t=1}^{N}u_t(\rho)\frac{\partial u_t}{\partial \rho}(\rho)\right] = 0 \tag{2.9}$$

If the gradient $\frac{\partial J}{\partial \rho}$ could be computed, then the solution of Equation (2.9) could be obtained by the following iterative algorithm:

$$\rho_{i+1} = \rho_i - \gamma_i {R_i}^{-1}\frac{\partial J}{\partial \rho}(\rho_i) \tag{2.10}$$

Here R_i is some appropriate positive definite matrix, typically a Gauss-Newton approximation of the Hessian of J, while γ_i is a positive real scalar that determines the step size. The sequence must obey some constraint for the algorithm to converge to

a local minimum of the cost function and is chosen to be

$$R_i = \frac{1}{N}\sum_{t=1}^{N}\left(\frac{\partial \tilde{y}_t}{\partial \rho}(\rho_i)\frac{\partial \tilde{y}_t}{\partial \rho}(\rho_i)^T + \lambda\frac{\partial u_t}{\partial \rho}(\rho_i)\frac{\partial u_t}{\partial \rho}(\rho_i)^T\right) \tag{2.11}$$

$$= \frac{1}{N}\sum_{t=1}^{N}\left(\frac{\partial y_t}{\partial \rho}(\rho_i)\frac{\partial y_t}{\partial \rho}(\rho_i)^T + \lambda\frac{\partial u_t}{\partial \rho}(\rho_i)\frac{\partial u_t}{\partial \rho}(\rho_i)^T\right) \tag{2.12}$$

From

$$y(\rho) = \frac{C(\rho)P}{1+C(\rho)P}r \tag{2.13}$$

we get

$$\frac{\partial y(\rho)}{\partial \rho} = \frac{1}{C(\rho)}\frac{\partial C(\rho)}{\partial \rho}\left[\frac{C(\rho)P}{1+C(\rho)P}(r - y(\rho))\right] \tag{2.14}$$

The term in the square bracket can be obtained by subtracting the plant output of one experiment on the closed-loop system from the original reference, and using this signal as the reference signal in a new experiment. The term in the square bracket is the plant output of the new experiment. This leads to the experiments in IFT: for each iteration i of the controller parameter ρ_i, two experiments are conducted. For a chosen N-length signal, r_s, the first experiment consists of setting the reference $r = r_s$and collecting the corresponding N samples of the plant output denoted as $y_1(\rho)$. The second experiment consists of setting reference $r = r_s - y_1(\rho)$ and collecting the corresponding N samples of the plant output denoted as $y_2(\rho)$.

$$\frac{\partial y(\rho)}{\partial \rho} = \frac{1}{C(\rho)}\frac{\partial C(\rho)}{\partial \rho}y_2(\rho) \tag{2.15}$$

In a similar way, the estimate of the sensitivity function $\frac{\partial u(\rho)}{\partial \rho}$ can be obtained as:

$$\frac{\partial u(\rho)}{\partial \rho} = \frac{1}{C(\rho)}\frac{\partial C(\rho)}{\partial \rho}u_2(\rho) \tag{2.16}$$

Then, $\frac{\partial J}{\partial \rho}$ in Equation (2.9) and ρ_{i+1}in Equation (2.10) can be computed.

The algorithm is summarized as follows:

With a controller $C(\rho)$ operating on the plant, generate the signals $y_1(\rho)$, $y_2(\rho)$, the signals $u_1(\rho)$, $u_2(\rho)$, and compute $\tilde{y}(\rho)$, $\frac{\partial y(\rho)}{\partial \rho}$, $\frac{\partial u(\rho)}{\partial \rho}$. Then the next controller parameters can be computed by Equation (2.10) where $\frac{\partial J}{\partial \rho}$ is given by Equation (2.9), where γ_i is a sequence of positive real numbers that determines the step size and where R_i is a sequence of positive definite matrices that are given by Equation (2.11).

2.5 Experimental results

A. Conventional Softbake

The resist thickness at two zones are monitored. The temperature is maintained at $90^o C$. As can be seen from Figure 2.7, at the beginning of the conventional softbake, the average resist thickness non-uniformity is around 100nm. At the end of the softbake, the non-uniformity is 93nm. On average, there is no significant change in thickness uniformity after conventional softbake.

B. IFT control of resist thickness

The experiment is conducted as follows. Prior to the experiment, one wafer is baked at $90^o C$ and the measured thickness is stored as y_r. For all the experiments, y_r is shifted down 100nm below the maximum resist thickness and used as the reference. By making the reference 100nm below the maximum thickness, we have assumed that the initial resist thickness non-uniformity among the two zones is less than 100nm. If the initial thickness non-uniformity is larger than this, the shift can be larger. The resist thickness of 2 zones are made to track the reference trajectory using *in situ* thickness sensors and IFT control algorithm. The reference trajectory would not vary too much if the coating process is repeatable. By making the reference 100nm below the maximum thickness, we have assumed that the initial thickness non-uniformity between 2 zones is less than 100nm. If the non-uniformity is larger than 100nm, the shift down can be larger. A PI controller $P(s) = K_P(1 + \frac{1}{sT_i})$ is used to control the thickness. 3 iterations of experiments are done and each iteration needs 2 experiments(namely Experiment A and Experiment B) in order to apply IFT

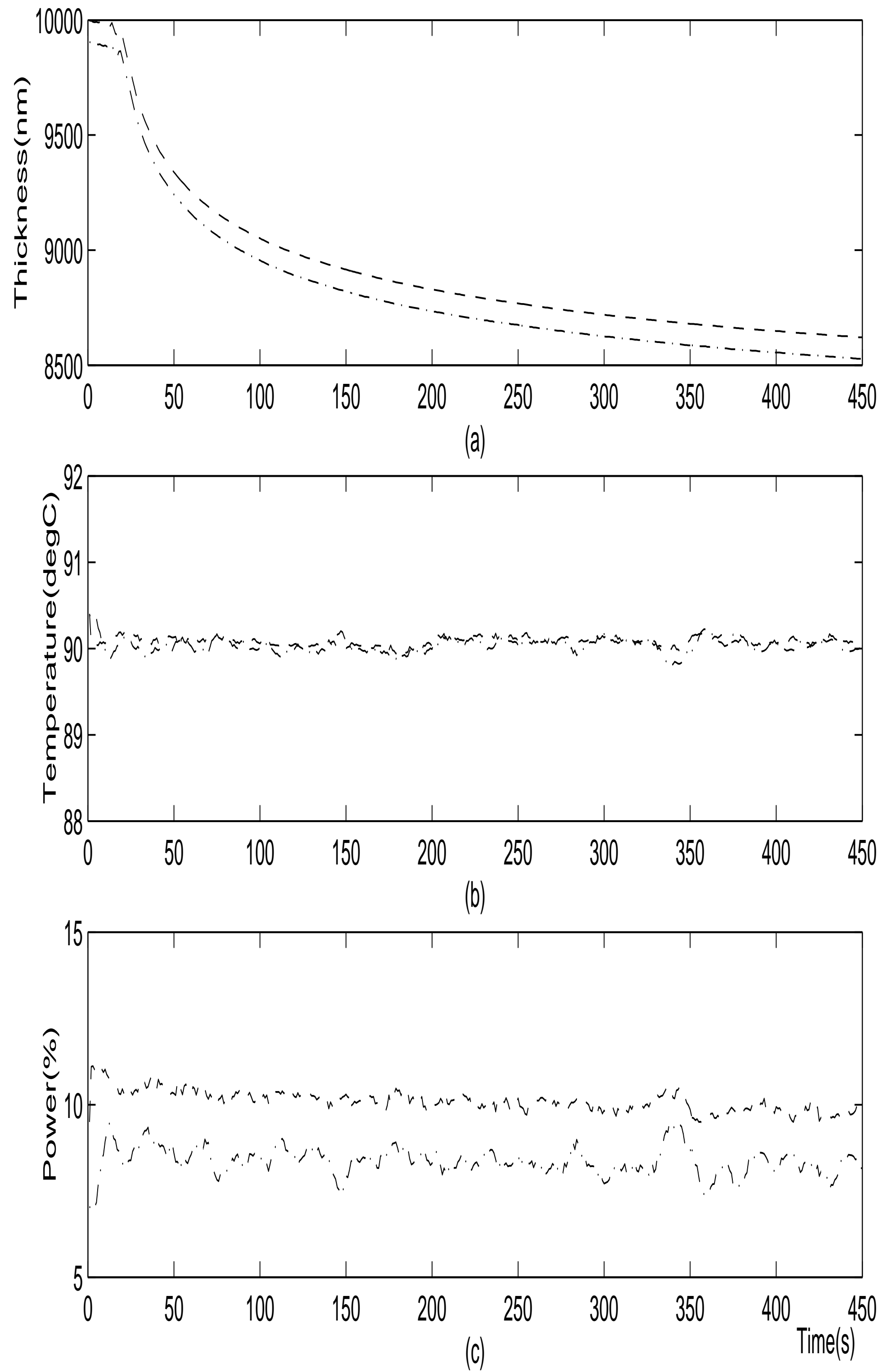

Figure 2.7. Conventional softbake with bakeplate maintained at 90^oC: zone 1 and zone 2 are represented by dashed and dashed-dotted lines respectively. (a)Thickness, (b)Temperature, (c)Power.

Table 2.1. Controller parameter, non-uniformity, and convergence time for Zone 1

	Experiment(1)	Experiment(2)	Experiment(3)
K_{P1}	5.0×10^6	5.4×10^6	5.7×10^6
T_{i1}	500	490	475
convergence time(seconds)	>400	231	172

Table 2.2. Controller parameter, non-uniformity, and convergence time for Zone 2

	Experiment (1)	Experiment (2)	Experiment (3)
K_{P2}	5.0×10^6	5.5×10^6	6.0×10^6
T_{i2}	500	423	400
convergence time(seconds)	>400	230	171

algorithm to update controller parameters. The criteria to stop the IFT update is that the update of K_P and T_i is within 5% for both zones. The first control move was made at $t = 0$. The thickness is considered converged to the reference when the difference between them is within 10nm.

Results of Experiment A for 3 iterations are presented in Figure 2.8.

In each iteration, after Experiment A is done, get the difference between the reference and output as the new reference of the Experiment B. Results of Experiment B for 3 iterations are shown in Figure 2.9.

In each iteration, after Experiment B is done, y_2 and u_2 are obtained. IFT algorithm can be used to update the parameters K_P and K_I of the controller. Choose $\lambda = 1.2$ and $\gamma = 0.07$ for both zones, and the PI parameters are updated to apply to the next iteration.

The controller parameters and the convergence time for zone 1 and zone 2 are summarized as Table 2.1 and Table 2.2 respectively.

After 3 iterations of experiments, the updated controller parameters K_{P1}, T_{i1}, K_{P2}, T_{i2} are 5.9×10^6, 453, 6.3×10^6 and 393 respectively.

The update of the controller parameters after the third iteration is summarized as follows:

$$K_{P1}\text{: } \frac{5.9 \times 10^6\text{-}5.7 \times 10^6}{5.7 \times 10^6} = 3.16\%;$$

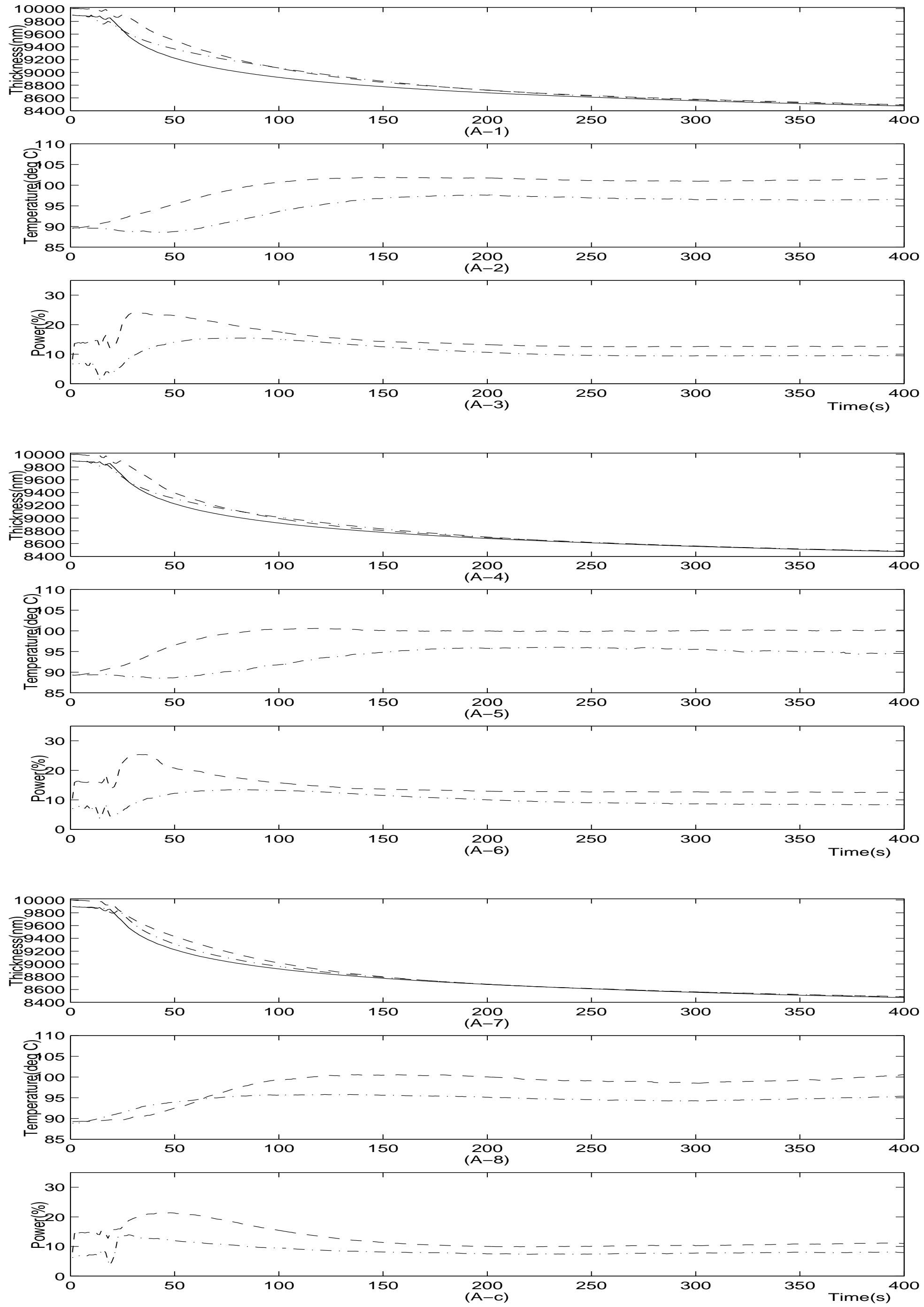

Figure 2.8. 3 iterations of Experiment A. (A-1) (A-4) (A-7) thickness, (A-2) (A-5) (A-8) temperature, (A-3) (A-6) (A-9) power. Two zones are monitored. Reference, zone 1 thickness measurement and zone 2 thickness measurement are represented by the solid, dashed and dashed-dotted lines respectively.

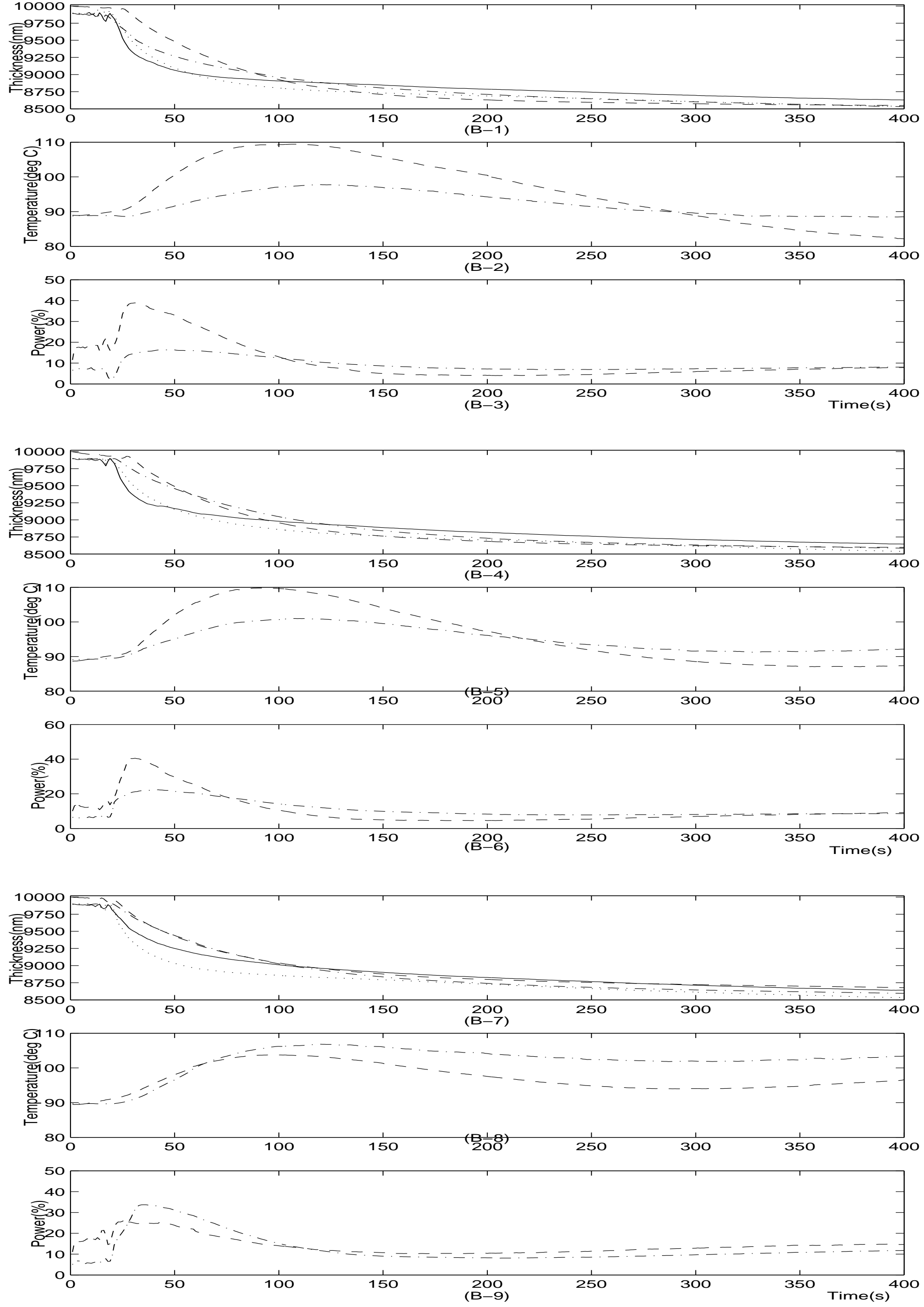

Figure 2.9. 3 iterations of Experiment B. (B-1) (B-4) (B-7) thickness, (B-2) (B-5) (B-8) temperature, (B-3) (B-6) (B-9) power. Two zones are monitored. Reference for zone 1, reference for zone 2, zone 1 thickness measurement and zone 2 thickness measurement are represented by the solid, dotted, dashed and dashed-dotted lines respectively.

Table 2.3. Summary of experiments. The first experiment is conventional softbake and the following 3 iterations of experiments are performed using the IFT approach

Bake Approach	Conventional Bake	Multizone-IFT Bake		
Iteration Number	0	1	2	3
Resist thickness non-uniformity before softbake(nm)	100	100	100	100
Resist thickness non-uniformity after softbake (nm)	93	6.8	7.5	6.4

Table 2.4. Improvement on the thickness uniformity

	t=25s	t=400s	improvement in uniformity
iteration 1	135.6658nm	7.5226nm	18.0344
iteration 2	114.6587nm	6.8007nm	16.8598
iteration 3	144.8847nm	6.3642nm	22.7656

$$T_{i1}\text{: } \frac{|453\text{-}475|}{475}\text{=4.63\%;}$$

$$K_{P2}\text{: } \frac{6.3\times10^6\text{-}6.0\times10^6}{6.0\times10^6}\text{=5\%;}$$

$$T_{i2}\text{: } \frac{|393\text{-}400|}{400}\text{=1.75\%;}$$

Since the update for all the controller parameters is within 5%, it satisfies the criteria to stop the IFT update, and iteration 3 should give the best result.

$$\text{Improvement in thickness uniformity}=\frac{\text{Initial thickness non-uniformity}}{\text{Final thickness non-uniformity}}$$

Table 2.3 and Table 2.4 summarize the result of IFT control.

In all these 3 iterations of experiments, the initial non-uniformity between zone 1 and zone 2 is obtained at t=25s when the thickness estimation is considered correct. The non-uniformity between zone 1 and zone 2 at the end of the softbake process is taken as the final thickness non-uniformity. The improvement in thickness uniformity is demonstrated in Table 2.4.

On average, there is 19× improvement in resist thickness uniformity with IFT.

2.6 Conclusions

In this chapter, thickness control has been implemented using an array of *in-situ* thickness sensors and an IFT control strategy. The PI controller is tuned using IFT during the experiment to give better resist thickness uniformity and a faster convergence to the reference. An average of 19× improvement in resist thickness uniformity has been obtained from wafer to wafer and across individual wafers, and a 1.7 times improvement in convergence time is achieved using IFT algorithm. The control strategy eliminates the need to get a precise model of the system to be controlled. It is simple and may be extended to similar applications.

Chapter 3

Relay auto-tuning of PID controllers using Iterative Feedback Tuning

3.1 Introduction

The Proportional-plus-Integral-plus-Derivative (PID) controllers have found wide acceptance and applications in the industries for the past few decades. However, it is given in Åström et al.(Åström et al, 1995) that audits of paper mills in Canada show that a typical mill has more than 2000 control loops and that 97% of them use PI control. Only 20% of the control loops were found to work well and decrease process variability. One of the reasons for poor performance was poor tuning(30%). Further comments on the performance and robustness of well-known PID tuning methods are given in Ho et al.(Ho et al, 1995b, 1996) and Åström et al.(Åström et al, 1993). There is a need for simple and effective tuning methods.

The technique of relay auto-tuning (Åström et al, 1984a-c, 1995; Hägglund et al, 1985; Li et al, 1991; Marchetti et al, 2000) of PID controllers has been proposed to automate the Ziegler-Nichols ultimate cycling tuning method (Ziegler et al, 1942). The standard relay auto-tuning uses a version of the Ziegler-Nichols tuning formula and therefore inherits its limitation: the Ziegler-Nichols tuning formula only gives

rough tuning. In practice, Ziegler-Nichols tuning has to be supplemented by manual fine-tuning (Hang et al, 1991; Ho et al, 1995b).

Iterative Feedback Tuning (IFT) (Hjalmarsson et al, 1994, 1995, 1998; Hansson et al, 1999; El-Awady et al, 1999; Lequin et al, 1999) is a technique inspired by iterative identification and control schemes. It is entirely driven by closed-loop data obtained on the actual closed-loop system operating under a sequence of controllers. The iterative control design scheme may be considered as a parameter optimization problem in which the optimization is carried directly on the controller parameters, thereby abandoning the step of identification of a model altogether.

In this chapter, ideas from IFT are incorporated into relay auto-tuning. The PID controller is auto-tuned to give specified phase margin and bandwidth. Good tuning performance according to the specified bandwidth and phase margin can be obtained and the limitation of the standard relay auto-tuning technique using a version of Ziegler-Nichols formula is eliminated. Furthermore, by using common modelling assumptions for the relay system, some of the required derivatives in the IFT algorithm can be derived analytically. In contrast, extra experiments are conducted to obtain these derivatives in the standard IFT algorithm because no such modelling assumptions are made.

The chapter is organized as follows. In Section 3.2, the idea of Iterative Feedback Tuning is presented. Realy auto-tuning is introduced in Section 3.3. The proposed IFT algorithm are discussed in Section 3.4. Discussions on the choices of phase margin and bandwidth are given in Section 3.5. Some examples on the implementation of IFT are shown in Section 3.6, and conclusions are drawn in Section 3.7.

3.2 Iterative Feedback Tuning

Consider Figure 3.1 where $C(s)$ and $P(s)$ are the controller and plant respectively. The signals r, u, and y are the reference, control and plant output respectively.

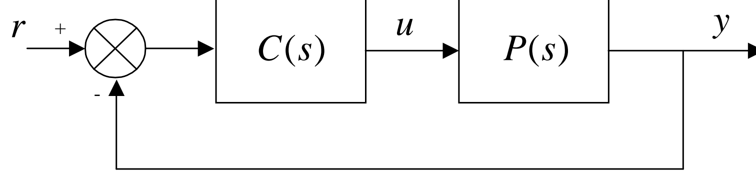

Figure 3.1. Conventional feedback system

A user-specified desired output y^d and a quadratic criterion

$$J(\rho) = \frac{1}{2N} \sum_{t=1}^{N} \tilde{y}_t(\rho)^2 \tag{3.1}$$

are defined where ρ, t, and N are the controller parameter, discrete time index and the number of samples considered respectively and $\tilde{y}_t(\rho) = y_t(\rho) - y_t^d$. A solution for ρ to the equation

$$\frac{\partial J(\rho)}{\partial \rho} = 0 \tag{3.2}$$

where

$$\frac{\partial J(\rho)}{\partial \rho} = \frac{1}{N} \sum_{t=1}^{N} \left(\tilde{y}_t(\rho) \frac{\partial \tilde{y}_t(\rho)}{\partial \rho} \right) = \frac{1}{N} \sum_{t=1}^{N} \left(\tilde{y}_t(\rho) \frac{\partial y_t(\rho)}{\partial \rho} \right) \tag{3.3}$$

would give the minimum of J. If the gradient $\frac{\partial J}{\partial \rho}$ could be computed, then the solution of Equation (3.2) could be obtained by the following iterative algorithm:

$$\rho_{i+1} = \rho_i - \gamma_i R_i^{-1} \frac{\partial J(\rho_i)}{\partial \rho} \tag{3.4}$$

Here R_i is some appropriate positive definite matrix

$$R_i = \frac{1}{N} \sum_{t=1}^{N} \left(\frac{\partial \tilde{y}_t(\rho_i)}{\partial \rho} \left[\frac{\partial \tilde{y}_t(\rho_i)}{\partial \rho} \right]^T \right) = \frac{1}{N} \sum_{t=1}^{N} \left(\frac{\partial y_t(\rho_i)}{\partial \rho} \left[\frac{\partial y_t(\rho_i)}{\partial \rho} \right]^T \right) \tag{3.5}$$

typically, a Gauss-Newton approximation of the Hessian of J, while γ_i is a positive real scalar that determines the step size.

From

$$y(\rho) = \frac{C(\rho)P}{1 + C(\rho)P} r$$

gives

$$\frac{\partial y(\rho)}{\partial \rho} = \frac{1}{C(\rho)} \frac{\partial C(\rho)}{\partial \rho} \left[\frac{C(\rho)P}{1 + C(\rho)P} (r - y(\rho)) \right]$$

The term in the square bracket can be obtained by subtracting the plant output of one experiment on the closed-loop system from the reference, and using this signal as the reference signal in a new experiment. The term in the square bracket is the plant output of the new experiment. This leads to the experiments in IFT: for each iteration i of the controller parameter ρ_i, two experiments are conducted. For a chosen N-length signal, r_s, the first experiment consists of setting the reference $r = r_s$ and collecting the corresponding N samples of plant output denoted as y_1. The second experiment consists of setting the reference $r = r_s - y_1$ and collecting the corresponding N samples of plant output denoted as y_2. The derivative required in Equation (3.3) is then computed as

$$\frac{\partial y(\rho_i)}{\partial \rho} = \frac{1}{C(\rho_i)} \frac{\partial C(\rho_i)}{\partial \rho} y_2(\rho_i) \tag{3.6}$$

and $\frac{\partial J(\rho_i)}{\partial \rho}$ in Equations (3.3) and (3.4) can be computed.

3.3 Relay Auto-Tuning

In relay auto-tuning, the relay is connected in the feedback loop as shown in Figure 3.2 to obtain limit cycle oscillation. The system is commonly analyzed using describing function (Åström and Hägglund, 1984a-c, 1995). From describing function theory, the limit cycle occurs at the point

$$N_L(a)G(j\omega) = -1 \tag{3.7}$$

and the oscillation at the process output can be approximated by

$$y = a \sin \omega t \tag{3.8}$$

where

$$N_L(a) = \frac{4h}{\pi a} \tag{3.9}$$

is the describing function of the relay and h and a are the amplitudes of the relay and oscillation at the plant output respectively.

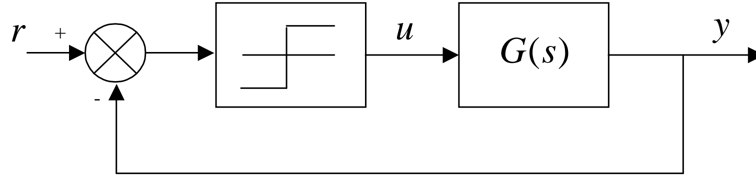

Figure 3.2. Relay Tuning

In conventional relay auto-tuning, the relay is connected directly to the plant, $P(s)$, i.e. $G(s) = P(s)$ in Figure 3.2. In the proposed tuning, the controller, $C(s)$, and a dead-time $D(s) = e^{-sL}$ are also inserted into the closed-loop ($G(s) = C(s)D(s)P(s)$ in Figure 3.2). The controller parameters will be tuned during the limit cycle such that the oscillation, y, at the plant output is made to track a given y^d. This can be done using Equations (3.3) and (3.4) as follows.

From Equations (3.7) and (3.9), the condition for limit cycle is now given as

$$\frac{4h}{\pi a} C(j\omega)D(j\omega)P(j\omega) = -1 \tag{3.10}$$

Equation (3.4) is used to update (tune) the controller parameters such that $J(\rho)$ in Equation (3.1) is minimised for a given y^d. To compute $\frac{\partial J}{\partial \rho}$ in Equation (3.3), $\frac{\partial y}{\partial \rho}$ has to be determined. From Equation (3.8)

$$\frac{\partial y}{\partial \rho} = \frac{\partial a}{\partial \rho} \sin \omega t + at \frac{\partial \omega}{\partial \rho} \cos \omega t \tag{3.11}$$

The derivatives $\frac{\partial a}{\partial \rho}$ and $\frac{\partial \omega}{\partial \rho}$ can be determined as follows. Equation (3.10) gives

$$\begin{aligned} a &= Re\left[-\frac{4h}{\pi}C(j\omega)D(j\omega)P(j\omega)\right] \\ \frac{\partial a}{\partial \rho} &= Re\left[-\frac{4h}{\pi}C(j\omega)D(j\omega)P(j\omega)\frac{\partial C(j\omega)}{\partial \rho}\frac{1}{C(j\omega)}\right] \end{aligned}$$

Using Equation (3.10),

$$\frac{\partial a}{\partial \rho} = Re\left[a\frac{\partial C(j\omega)}{\partial \rho}\frac{1}{C(j\omega)}\right] \tag{3.12}$$

Consider the PID controller:

$$C(s) = K_C^{'}\left(1 + \frac{1}{sT_I} + sT_D\right) \tag{3.13}$$

If for simplicity, we use the Ziegler-Nichols (1942) formula of $T_D = \frac{T_I}{4}$ then

$$C(s) = \frac{K_C^{'}}{sT_I}\left(1 + s\frac{T_I}{2}\right)^2 = \frac{K_C}{s}\left(1 + s\frac{T_I}{2}\right)^2 \tag{3.14}$$

and $\frac{\partial a}{\partial \rho}$ and $\frac{\partial \omega}{\partial \rho}$ in Equation (3.11) can be found as follows. Substituting Equation (3.14) into Equation (3.12) and letting $\rho = K_C$ in Equation (3.12), we get:

$$\frac{\partial a}{\partial K_C} = \frac{a}{K_C} \tag{3.15}$$

Similarly substituting Equation (3.14) into Equation (3.12) and letting $\rho = T_I$ in Equation (3.12), we get:

$$\frac{\partial a}{\partial T_I} = \frac{2a\omega^2 T_I}{4 + \omega^2 T_I^2} \tag{3.16}$$

Substituting Equation (3.14) into Equation (3.10), we get:

$$\begin{aligned} \frac{4h}{\pi a}\frac{K_C}{j\omega}\left(1 + j\omega\frac{T_I}{2}\right)^2 D(j\omega)P(j\omega) &= -1 \\ arg\left[\frac{1}{j\omega}\left(1 + j\omega\frac{T_I}{2}\right)^2 D(j\omega)P(j\omega)\right] &= -\pi \end{aligned} \tag{3.17}$$

The frequency ω can be determined from Equation (3.17) which is independent of K_C. Therefore

$$\frac{\partial \omega}{\partial K_C} = 0 \tag{3.18}$$

The partial derivative $\frac{\partial \omega}{\partial T_I}$ may be approximated during the relay experiment as

$$\frac{\partial \omega}{\partial T_I} \approx \frac{\omega_i - \omega_{i-1}}{T_{Ii} - T_{I(i-1)}} \tag{3.19}$$

where ω_{i-1} and ω_i are the angular frequencies of the previous and current half-cycles of the relay oscillation respectively. Similarly, $T_{I(i-1)}$ and T_{Ii} are the integral times of the PID controller at the previous and current half-cycles of the relay oscillations respectively. Finally, $\frac{\partial y}{\partial \rho}$ of Equation (3.3) can be determined as follows. Letting $\rho = K_C$ in Equation (3.11) and substituting for $\frac{\partial a}{\partial K_C}$ (Equation 3.15) and $\frac{\partial \omega}{\partial K_C}$ (Equation 3.18), we get:

$$\frac{\partial y}{\partial K_C} = \frac{a}{K_C} \sin \omega t \tag{3.20}$$

Similarly, letting $\rho = T_I$ in Equation (3.11) and substituting for $\frac{\partial a}{\partial T_I}$ (Equation 3.16) and $\frac{\partial \omega}{\partial T_I}$ (Expression 3.19), we get:

$$\frac{\partial y}{\partial T_I} \approx \frac{2a\omega^2 T_I}{4 + \omega^2 T_I^2} \sin \omega t + at \frac{\omega_i - \omega_{i-1}}{T_{Ii} - T_{I(i-1)}} \cos \omega t \tag{3.21}$$

3.4 The Proposed Algorithm

The key idea is given as follows. Phase margin, ϕ_m, and bandwidth, ω_b, are common design parameters for control systems given in standard text(Franklin et al, 2002). The bandwidth, ω_b, is defined here as the frequency where the Nyquist curve of $C(j\omega)P(j\omega)$ has a magnitude of 1). Specifying $y^d = \frac{4h}{\pi} \sin \omega_b t$ and adding a controller $C(s)$ and dead-time $D(s) = e^{-sL}$ in the loop gives $G(s) = C(s)P(s)e^{-sL}$ in Figure 3.2. If the limit cycle, $y = a \sin \omega t$, of Equation (3.8) tracks y^d, then $a = \frac{4h}{\pi}$, $\omega = \omega_b$,

and Equation (3.9) gives $N_L(a) = 1$. Equation (3.7) now gives

$$C(j\omega_b)P(j\omega_b)e^{-j\omega_b L} = -1$$
$$\omega_b L = \pi + arg[C(j\omega_b)P(j\omega_b)]$$

Using the definition of phase margin

$$\phi_m = \pi + \arg[C(j\omega_b)P(j\omega_b)] \tag{3.22}$$

gives $\phi_m = \omega_b L$.

Here, the dead-time $D(s) = e^{-sL}$ is added because it's required to enable the free choice of ϕ_m as $\phi_m = \omega_b L$. Without the insertion of the dead-time, the phase margin ϕ_m can only be zero, which rules out any other free choice of phase margin.

The implementation algorithm can now be given.

1. Specify the phase margin (ϕ_m), bandwidth (ω_b) and desired output ($y^d = \frac{4h}{\pi}\sin\omega_b t$).
2. Run the standard relay experiment to obtain the ultimate gain, K_u, and ultimate frequency, ω_u.
3. Insert a PID controller using Ziegler-Nichols (1942) tuning.
4. Insert dead-time of L into the loop where $L = \frac{\phi_m}{\omega_b}$.
5. Collect the signal y_t. After the i half-cycle of the relay oscillation, if y_t has not converged to y_t^d, then from the data collected in the i half-cycle:
   (a) compute $\tilde{y}_t = y_t - y_t^d$.
   (b) compute ω, the angular frequency of the i half-cycle.
   (c) compute $\frac{\partial y}{\partial K_C}$ (Equation 3.20), $\frac{\partial J}{\partial K_C}$ (Equation 3.3) and $K_{C(i+1)}$ (Equation 3.4)
   (d) compute $\frac{\partial y}{\partial T_I}$ (Equation 3.21), $\frac{\partial J}{\partial T_I}$ (Equation 3.3) and $T_{I(i+1)}$ (Equation 3.4)

(e) update the PID parameters with $K_{C(i+1)}$ and $T_{I(i+1)}$.

(f) Repeat Step 5 for $i = i + 1$.

else

(a) remove the relay and dead time of L

If the problem is that of re-tuning or fine-tuning of an existing PID controller, then Step 2 and 3 may be skipped. The resultant PID tuning will give a system with the specified phase margin ϕ_m and bandwidth ω_b. Since the algorithm only requires two specifications, only two of the three PID parameters (K_c, T_I, T_D) can be tuned independently. For simplicity, we have chosen the commonly used ratio of $T_D = T_I/4$ to give two independent PID parameters. The algorithm will work for other ratios.

It should be noted that there is a difference between the approach taken in this chapter and the standard IFT method. This chapter presents a model based approach where the common modelling assumptions for relay systems in limit cycle are used. This amounts to (i) the signal at the process output is a sinusoid (Equation 3.8) and (ii) the describing function expression (Equation 3.10) holds. Based on these assumptions, the derivatives of the output with respect to the controller parameter (Equations 3.15, 3.16, 3.18, 3.20) can be derived analytically. In contrast, because no such modelling assumptions are made, two experiments for each iteration have to be conducted in the IFT method to collect y_2 to compute the derivatives using Equation (3.6).

3.5 Choices of Phase Margin and Bandwidth

Recommended choice of ϕ_m is usually between 30° to 60°. The bandwidth, ω_b, however should be chosen taking into account the open-loop dynamics and the specified phase margin ϕ_m. Guidelines on the choice of the bandwidth, ω_b, can be given by considering the typical case of Ziegler-Nichols (1942) tuning of the PID controller in Equation

(3.13):

$$\begin{aligned} K_C^{'} &= 0.6K_u \\ T_I &= 0.5T_u = \frac{\pi}{\omega_u} \\ T_D &= 0.125T_u \end{aligned} \tag{3.23}$$

for a second-order plus dead-time plant:

$$P(s) = \frac{K_p e^{-sd}}{(sT+1)^2}$$

where K_u and T_u are the ultimate gain and ultimate period which can be obtained from the standard relay experiment. Using pade approximation for the dead-time gives

$$P(s) = \frac{K_p}{(sT+1)^2}\frac{1-0.5sd}{1+0.5sd} \tag{3.24}$$

The ultimate gain, K_u, and ultimate frequency, ω_u, which defines the point where the nyquist curve of $P(s)$ crosses the negative real axis, are given as

$$|P(j\omega_u)| = \frac{K_p}{(\omega_u T)^2+1} = \frac{1}{K_u} \tag{3.25}$$

$$\arg[P(j\omega_u)] = -2\arctan(\omega_u T) - 2\arctan\left(\frac{\omega_u d}{2}\right) = -\pi \tag{3.26}$$

Express the bandwidth ω_b as a ratio of the ultimate frequency, ω_u:

$$z = \frac{\omega_b}{\omega_u} \tag{3.27}$$

Using Equation (3.27) and substituting for $P(s)$ from (3.24) and $C(s)$ from Equation (3.14) and (3.23) into the definition of phase margin in Equation (3.22) gives

$$\phi_m = \frac{\pi}{2} - 2\arctan(z\omega_u T) - 2\arctan\left(\frac{1}{2}z\omega_u d\right) + 2\arctan\left(\frac{1}{2}z\pi\right)$$

which can be simplified to

$$\left[\frac{\omega_u^2 T d\pi}{4}\right] z^3 + \alpha \left[\frac{\omega_u^2 T d}{2} - \frac{\pi}{2}\left(w_u T + \frac{w_u d}{2}\right)\right] z^2 + \left[\omega_u T + \frac{\omega_u d}{2} - \frac{\pi}{2}\right] z - \alpha = 0 \quad (3.28)$$

where $\alpha = \tan\left(\frac{\pi}{4} - \frac{\phi_m}{2}\right)$. Equation (3.28) is a third-order equation and can be solved analytically. The time-constant, T, can be obtained from Equation (3.25) and is given as $T = \frac{1}{\omega_u}\sqrt{K_u K_p - 1}$. Before the experiment, the static gain, K_p, can be obtained by making a small setpoint change. The dead-time, d, can be obtained from Equation (3.26) and is given as $d = \frac{2}{\omega_u}\tan(\frac{\pi - 2\arctan(\omega_u T)}{2})$. The smallest positive real root of z is a good default value for the ratio between ω_b and ω_u. In practice, the exact computed value need not be used, any value around it will do. If the default ratio, z, is to be used, then ω_b need not be specified in Step 1 of the algorithm. After Step 2, ω_u is known and z can be computed from Equation (3.28) and used in Step 4 of the algorithm.

3.6 Examples

Some examples will clarify matters. The diagram for the tuning experiments is shown in Figure 3.3. It includes the plant $P(j\omega)$, the relay, a noise filter $C(j\omega)$, a dead-time $e^{-j\omega_b L}$ and a switch. For implementation purposes, it is typical to include a noise filter for the derivative term in the PID control law (Åström and Wittenmark, 1997)

$$C(s) = K_C^{'}\left(1 + \frac{1}{sT_I} + \frac{sT_D}{sT_D/10 + 1}\right)$$

and this is used in the examples. For all the simulation examples, the specification $\phi_m = 60°$; the amplitude of the relay was chosen as $h = 1$; R_i was chosen according to Equation (3.5) and $\gamma_i = 0.5$. For simplicity, y was considered to have converged if the time interval and amplitude of a given half-cycle were within 10% of those of y^d.

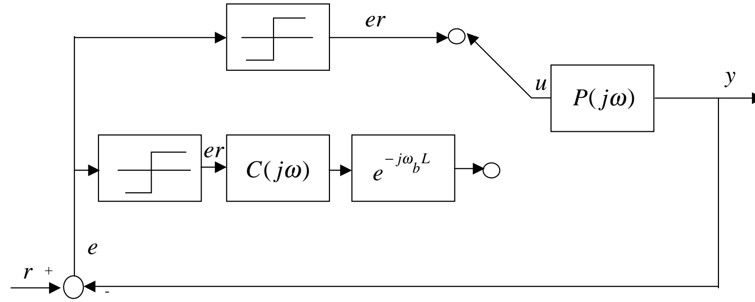

Figure 3.3. Diagram for the relay auto-tuning experiment

Simulation Example

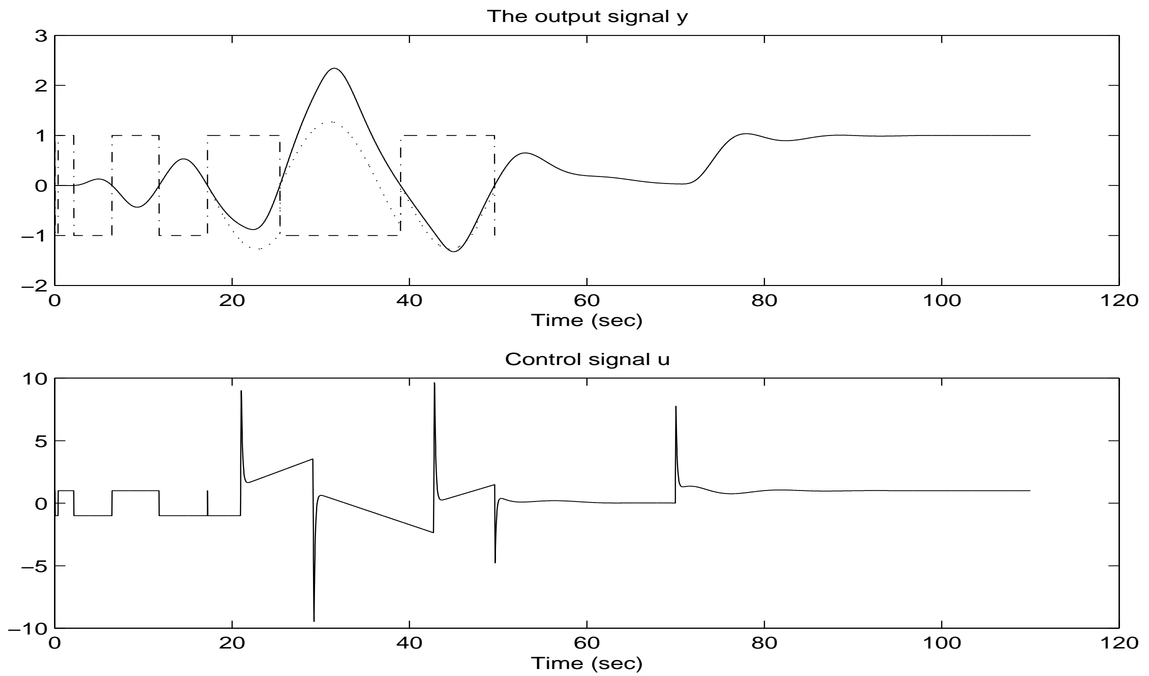

Figure 3.4. Iterative Feedback Tuning. $P(s) = \frac{1}{(s+1)^6}$; y^d: dotted line; er: dashed line

Consider a sixth order plant

$$P(s) = \frac{1}{(s+1)^6}$$

The simulation result is shown in Figure 3.4. The standard relay experiment was performed from $t = 0s$ to $18s$ where the ultimate gain $K_u = 2.4$ and ultimate period $T_u = 10.9s$ ($\omega_u = 0.58$) were determined. Equation (3.28) gives $z = 0.49$ ($\omega_b = z \times \omega_u = 0.29$). A dead-time of $L = \frac{\phi_m}{\omega_b} = 3.7s$ and a PID controller with Ziegler-

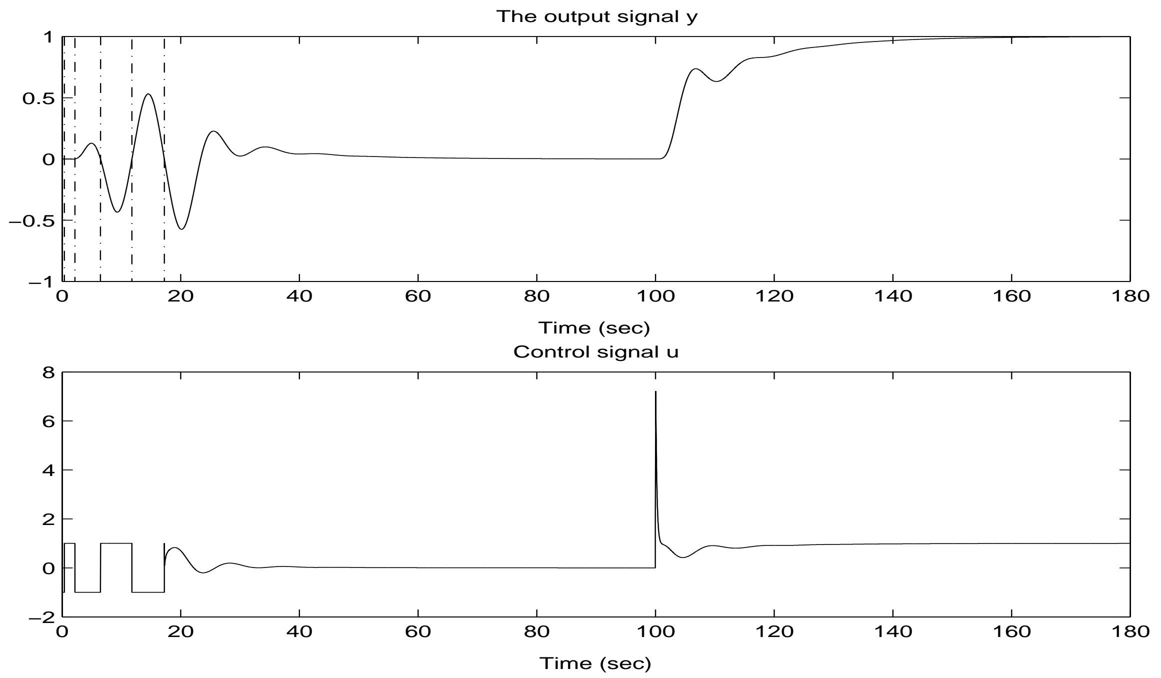

Figure 3.5. Tuning result of Equation (3.29)

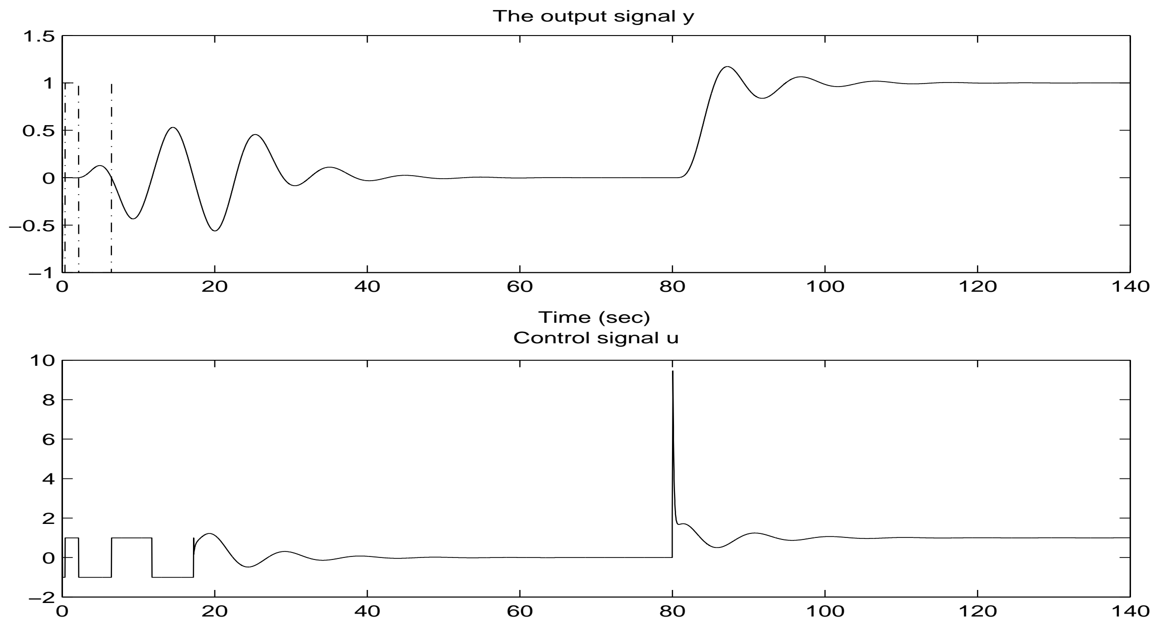

Figure 3.6. Ziegler-Nichols tuning

Nichols tuning of Equation (3.23) were inserted into the loop at $t = 18s$. The reference trajectory $y^d = \frac{4}{\pi}\sin(0.29t)$ was chosen. After the oscillations converged at $t = 50s$, the relay and dead-time of L were removed. The step response at $t = 72s$ was good. After tuning, the PID parameters were $K_C' = 1.3$, $T_I = 5.3$, $T_D = 1.3$ and the phase margin and bandwidth were about 65° and 0.29 respectively. If the problem is that of fine-tuning of an existing PID controller then the first part ($0s$ to $18s$) of the relay experiment may not be necessary.

Figure 3.5 shows the relay experiment with the design method and specification in Åström and Hägglund (1984a-c) where it is required that the Nyquist curve intersects the circle with radius 0.5 at an angle of 135°. The design equations are given as

$$\begin{aligned} T_i &= \alpha T_d \\ T_d &= \frac{\tan\phi_m + \sqrt{\frac{4}{\alpha} + \tan^2\phi_m}}{2\omega_u} \\ K_c &= r_s K_u \cos\phi_m \end{aligned} \tag{3.29}$$

where $\alpha = 4$, $\phi_m = 45°$, $r_s = 0.5$.

Figure 3.6 shows the relay experiment with the Ziegler-Nichols tuning. The settling time for the step response in Figures 3.4, 3.5 and 3.6 are about 15s, 40s and 30s respectively. A better performance of settling time of 15s can be obtained in Figure 3.4 because of better PID controller tuning. This is possible because of the extra relay oscillations from t=18 to 50 where more information of the plant model is extracted and made use of.

Implementation Example

The algorithm was tested in the laboratory on a coupled-tank as shown in Figure 3.7. The controlled variable was the liquid level, y.

The phase margin specification was given as $\phi_m = 60°$. The initial amplitude of the relay was chosen as $h = 0.1$ but will be adjusted in the course of the experiment to control the amplitude of the oscillations at the plant output (Åström and Hägglund, 1984a-c, 1995; Hägglund and Åström, 1985). The result is shown in Figure 3.8. The

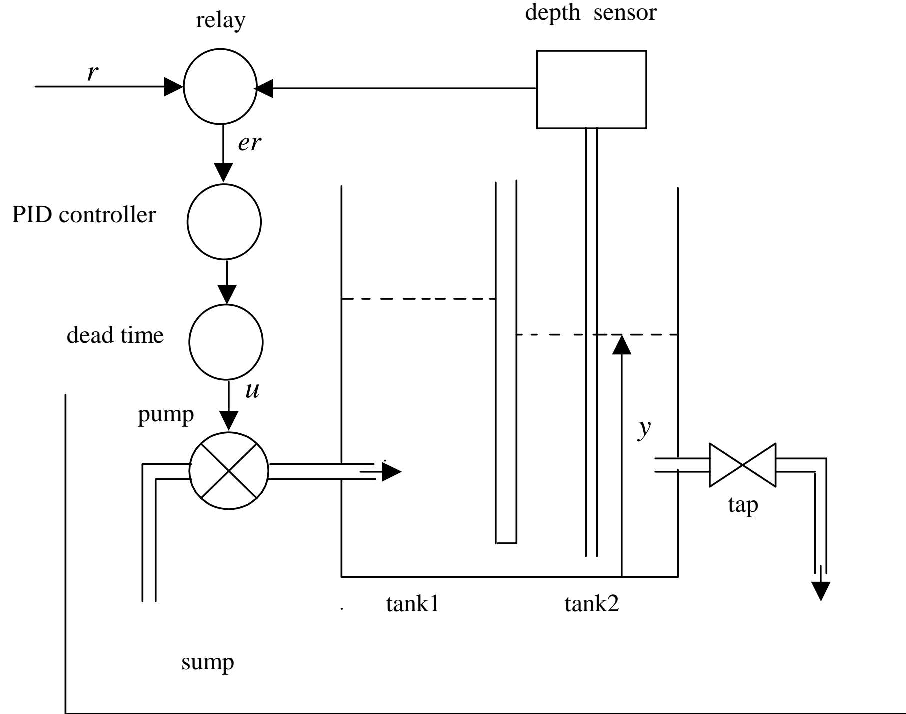

Figure 3.7. Coupled-tanks system

standard relay experiment was performed from $t = 0s$ to $40s$ where the ultimate gain $K_u = 7.1$ and ultimate period $T_u = 26s$ ($\omega_u = 0.24$) were determined. Equation (3.28) gave $z = 0.11$ ($\omega_b = z \times \omega_u = 0.03$).

A deadtime of $L = \frac{\phi_m}{\omega_b} = 40s$ and the PID controller were inserted into the loop at $t = 40s$. The PID controller initialized with Ziegler-Nichols tuning of Equation (3.23) gave very large oscillation amplitude (about 100%) for the first half-cycle immediately after the insertion of the PID controller. In this example, we have retained Ziegler-Nichols tuning for T_I and T_D but detuned K_C' ($K_C' = 0.1K_u$) to give a more manageable oscillation amplitude for the first half-cycle.

The oscillations converged at $t = 1100s$ and the step response at $t = 2050s$ was good. The new PID parameters were $K_C' = 0.1$, $T_I = 13$, $T_D = 3.3$. The reference trajectory $y^d = 0.49 + \frac{0.2}{\pi}\sin(0.12t)$ was chosen. R_i was chosen according to Equation (3.5) and $\gamma_i = 0.5$.

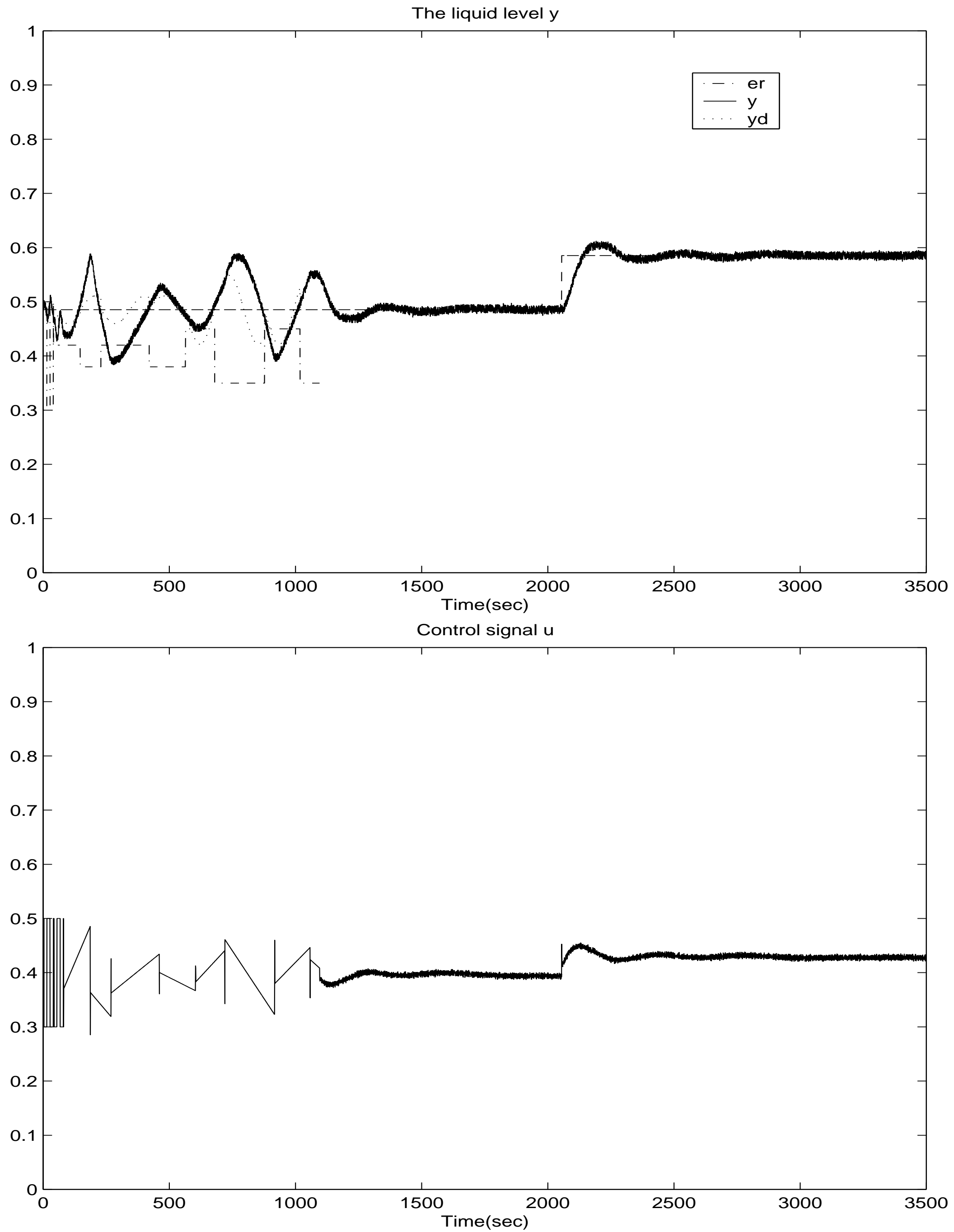

Figure 3.8. Real-time experimental result

3.7 Conclusions

In this chapter, the PID controller is auto-tuned during the relay experiment using IFT technique to give specified phase margin and bandwidth. Good tuning per-

formance according to the specified bandwidth and phase margin can be obtained and the limitation of the standard relay auto-tuning technique using a version of the Ziegler-Nichols formula can be eliminated. The algorithm was tested in the laboratory on a coupled-tank and good tuning result was demonstrated. As opposed to the standard IFT algorithm, a number of the derivatives required in the algorithm are obtained analytically with this proposed method.

Chapter 4

Conclusions

4.1 Main Findings

The trend in the semiconductor industry is towards the use of more advanced process control methods to meet the tightening process specifications with the continual shrinking of the feature sizes(CDS panel report, 2002). This thesis examines the application of iterative feedback tuning algorithm to meet the challenges of some aspects of advanced lithography, particularly on the softbake process. Also, IFT algorithm is applied to relay auto-tuning of PID controllers. In this section, some results are summarized. The scope for future developments is proposed in the next section.

In Chapter 2, a thickness control strategy using IFT is implemented for the softbake process to achieve good resist thickness uniformity across the wafer and from wafer-to-wafer. The approach is to use an array of in-situ thickness sensors positioned above a multi-zone bakeplate to monitor the resist thickness. With these in-situ thickness measurements, the temperature profile is controlled by manipulating the heater power distribution using suitable control algorithm. The PI controller is updated after each iteration of experiment. After 3 iterations, an average of $19\times$ improvement in resist thickness uniformity has been obtained, and a 1.7 times improvement in convergence time is achieved using IFT algorithm. The control strategy eliminates the need to get a precise model of the system to be controlled. It is simple and may be extended to similar applications.

However, the IFT in resist thickness control needs two experiments for each iteration in order to get the input/output data and compute the derivatives. In Chapter 3 of the thesis, we investigate the application of IFT in the relay auto-tuning of PID controllers, which presents a model-based approach where the common modelling assumptions for relay systems in limit cycle are used. Based on these model assumptions for the relay system, the derivatives of the output with respect to the controller parameter can be derived analytically, thus eliminating the need of the second experiment in each iteration. The PID controller is auto-tuned during the relay experiment to give specified phase margin and bandwidth. Good tuning performance can be obtained. The algorithm was tested in the laboratory on a coupled-tank and good tuning result was demonstrated.

4.2 Suggestions for Further Work

The focus of this thesis is on the IFT control of the bake process involved in lithography. The same experimental setup and control strategy can be extended to the development process. This is because the development process is also a strong function of temperature. In order to implement this for the development process, it is important to be able to monitor the development process on-line. While commercial development rate monitor is available, a more advanced data analysis is required to estimate the resist thickness from the reflectance signals during development. This is because reflectance signal used for resist thickness measurement may be distorted due to the topography of wafers, absorbing resist residue in developer, developer layer and many other factors(Michael *et al*, 1989). Given that the development process is the last step in forming the resist patterns, the ability to control the development process through IFT can reduce variations.

IFT can also be extended to control the CD(Critical Dimension) since CD is a function of resist thickness. Similarly, the resist thickness can be manipulated by IFT so that a non-uniform resist film can give rise to a more uniform CD distribution. This can help to compensate for CD variation caused by variations of other process variables.

Bibliography

Åström, K. J and Hägglund T. (1984a). Automatic tuning of simple regulators. *Proceedings of the 9th IFAC World Congress, Budapest, Hungary.* pp. 1867–1872.

Åström, K. J and Hägglund T. (1984b). Automatic tuning of simple regulators with specifications on phase and amplitude margins. *Automatica,* **vol. 20**, pp. 645–651.

Åström, K. J and Hägglund T. (1984c). A frequency domain approach to automatic tuning of simple feedback loops. *Proceedings of the 23rd IEEE conference on decision and control, Las Vegas, Nevada, USA.* pp. 299–304.

Åström, K. J and Hägglund T. (1995). *PID Controllers: Theory, Design, and Tuning.* Instrument Society of America. NC, USA.

Åström, K. J and Wittenmark B. (1997). *Computer-Controlled Systems, 3rd ed.* Prentice Hall.

Åström K. J, Hägglund T, Hang C.C and Ho W.K. (1993). Automatic tuning and adaptation for PID controllers—a survey. *CEP,* **vol. 1**(4), pp. 699–714.

A.B.Charles, J.G. Matlabes, S.R. Horing T.S. Schedel D. Ganz S. Schmidt L. Grant G. Hraschan K.E. Mautz and R. Otto (1999). Current state of 300mm lithography in pilot line environment. *Proceedings of SPIE,* **vol. 3882**, pp. 140.

Born, M. and E. Wolf (1980). *Principles of Optics.* Pergamon. Oxford, U.K.

Brunner, T. A. (1991). Optimization of optical properties of resist processes. *Proceedings of SPIE,* **vol. 1466**, pp. 297–308.

C. D. Schaper, K. El-Awady and A.Tay (1999). Spatially programmable temperature control and measurement for chemically amplified photoresist processing. *Proceedings of SPIE,* **vol. 3882**, pp. 74–79.

C. L. Henderson, S. A. Sheer, P. C. Tsiatas B. M. Rathsack J. P. Sagan R. R. Dammel A. Erdmann and C. G. Willson (1998). Modeling parameter extraction for DNQ-novolac thick film resist. *Proceedings of SPIE,* **vol. 3333**, pp. 256–267.

Control in an Information Rich World (2002). *Report of the Panel on Future Directions in Control, Dynamics, and Systems, USA*.

E. Fadda, C. Clarisse and P. J. Paniez (1996). Study of bake mechanisms in novolak based photoresist films: Investigation by contact angle measurements. *Proceedings of SPIE,* **vol. 2714**, pp. 460–468.

E. Gurer, T. Zhong, J. Lewellen and E. Lee (2000). A novel spon coating technology for 248nm/193nm duv lighography and low-k spin on dielectrics of 200/300mm wafers. *Proceedings of SPIE,* **vol. 3999**, pp. 805–817.

El-Awady, K. (2000). Spatially programmable thermal processing module for semiconductors. *Ph.D dissertation, Stanford University, CA, USA*.

El-Awady K., A Hansson and B. Wahlberg (1999). Application of iterative feedback tuning to a thermal cycling module. *Proceedings of the 14th World Congress of IFAC, Invited Session, Beijing, P.R. China.*

Fowles, G. R. (1975). *Introduction to Modern Optics*. New York:Dover. USA.

Franklin G. F, Powell J. D and Emami-Naeini A (2002). *Feedback control of dynamic systems, 4th ed*. Prentice Hall. Englewood Cliffs, NJ, USA.

Gunnarsson S., Rousseaux O. and Collignon V. (1999). Iterative feedback tuning applied to robot joint controllers. *The 14th World Congress of IFAC, Beijing, P.R. China.* pp. 451–456.

Hägglund T., Åström, K. J. (1985). Method and an apparatus in tuning a PID regulator. *US patent No.4549123*.

Hang C. C., Åström, K. J. and W. K. Ho (1991). Refinements of the ziegler-nichols tuning formula. *IEE,* **vol. 138**(2), pp. 111–118.

Hansson A., K. El-Awady, B. Wahlberg (1999). A primal-dual interior-point method for iterative feedback tuning. *Proceedings of The 14th World Congress of IFAC, Invited Session, Beijing, China.* pp. 427–431.

Hjalmarsson, H. (1998). Control of nonlinear systems using iterative feedback tuning. *1998 American Control Conference, Philadelphia, USA.*

Hjalmarsson H., Birkeland, T. (1998). Iterative feedback tuning of linear time-invariant mimo systems. *37th IEEE Conference on Decision and Control, Tampa, USA.* pp. 3893–3898.

Hjalmarsson H., Cameron M. T. (1999). Iterative feedback tuning of controllers in cold rolling mills. *The 14th World Congress of IFAC, Beijing, P.R. China.* pp. 445–450.

Hjalmarsson H., Gevers M. and Lequin O (1998). Iterative feedback tuning: Theory and applications. *IEEE Control Systems Magazine,* **vol. 4**(18), pp. 24–41.

Hjalmarsson H., Gunnarsson S. and Gevers M. (1994). A convergent iterative restricted complexity control design scheme. *Proceedings of 33rd IEEE Conference on Decision and Control, Florida, USA.* pp. 1735–1740.

Hjalmarsson H., Gunnarsson S. and Gevers M. (1995). Optimality and sub-optimality of iterative identification and control design schemes. *American Control Conference, Seattle, Washington, USA.*

Ho, W. K., Gan O. P. Tay E.B. and E. L. Ang (1996). Performance and gain and phase margins of well-known PID tuning formulas. *IEEE Transactions On Control Systems Technology,* **vol. 4**(4), pp. 473–477.

Ho, W.K., A. Tay and C.D. Schaper (2000). Optimal predictive control with constraints for the processing of the semiconductor wafers on large thermal-

mass heating plates. *IEEE Transactions on Semiconductor Manufacturing,* **vol. 13**, pp. 88–96.

Ho, W.K., Hang C.C. and J.H Zhou (1995a). Performance and gain and phase margins of well-known PI tuning formulas. *IEEE Transactions On Control Systems Technology,* **vol. 3**(2), pp. 245–248.

Ho, W.K., Hang C.C. and L.S Cao (1995b). Tuning of PID controllers based on gain and phase margin specifications. *Automatica,* **vol. 31**(3), pp. 497–502.

Ho W.K., Lay Lay Lee, Arthur Tay and Charles Schaper (2002). Resist film uniformity in the microlithography process. *IEEE Transactions on Semiconductor Manufacturing,* **vol. 15**(3), pp. 323–330.

International Technology Roadmap for Semiconductors: Lithography (1999). Semiconductor Industry Association.

L. L. Lee, C. D. Schaper and W. K. Ho (2000). Real-time control of photoresist thickness uniformity during the bake process. *Proceedings of SPIE,* **vol. 4182**, pp. 54–64.

Lay Lay Lee, Charles D. Schaper and Weng Khuen Ho (2002). Real-time predictive control of photoresist film thickness uniformity. *IEEE Transactions On Semiconductor Manufacturing,* **vol. 15**(1), pp. 51–59.

Lequin O., Gevers M. and Triest L (1999). Optimizing the settling-time with iterative feedback tuning. *The 14th World Congress of IFAC, Invited Session, Beijing, P.R. China*.

Levison, H. J. (1999). *Lithography Process Control.* SPIE Optical Press. Bellingham, Washington, USA.

Li, W., Eskinat E. and Luyben W. L. (1991). An improved autotune identification method. *Industrial and Engineering Chemistry Research,* **vol. 30**, pp. 1530–1541.

M. C. Campi, A. Lecchini, S. M. Savaresi (2002). Virtual reference feedback tuning:a direct method for the design of feedback controllers. *Automatica,* **vol. 38**(8), pp. 1337–1346.

Marchetti (1999). *International Technology Roadmap for Semiconductors: Lithography*. Semiconductor Industry Association.

Marchetti, G. and C. Scali (2000). Use of modified relay techniques for the design of model-based controllers for chemical processes. *Industrial and Engineering Chemistry Research,* **vol. 39**, pp. 3325–3334.

Morton, S. L. (1999a). Ultrasonic sensor for photoresist process monitoring. *Ph.D. dissertation, Stanford Univ., Stanford, CA, USA*.

P. J. Paniez, A. Vareille, P. Ballet and B. Mortini (1998). Study of bake mechanisms by real-time in-situ ellipsometry. *Proceedings of SPIE,* **vol. 3333**, pp. 289–300.

Palmer E., W. Ren, C. J. Spanos and K.Poolla (1996). Control of photoresist properties: A Kalman filter based approach. *IEEE Transactions On Semiconductor Manufacturing,* **vol. 9**(2), pp. 208–214.

S. L. Morton, F. L. Degertekin and B. T. Khuri-Yakub (1999b). Ultrasonic monitoring of photoresist processing. *Proceedings of SPIE,* **vol. 3677**, pp. 340–347.

Sheats, J. R. and B. W. Smith (1998). *Microlighography:Science and Technology*. New York:Marcel Dekker, USA.

T. E. Metz, R. N. Savage and H. O. Simmons (1991). In-situ film thickness measurements for real-time monitoring and control of advanced photoresist track coating systems. *Proceedings of SPIE,* **vol. 1594**, pp. 146–152.

T. L. Vincent, P. P. Khargonekar and F. L. Terry Jr (1997). An extended kalman filtering-based method of processing reflectometry data for fast in-situ etch rate measurements. *IEEE Transactions On Semiconductor Manufacturing,* **vol. 10**(1), pp. 42–51.

Ziegler, J. G. and N. B Nichols (1942). Optimum setting for automatic controllers. *Transactions of the ASME,* **vol. 64**, pp. 759–768.

Author's Publications

List of publications

[1] W.K. Ho, Y. Hong, A. Hansson, H. Hjalmarsson, J.W. Deng, Relay auto-tuning of PID controllers using iterative feedback tuning, Automatica 39 (2003), pp. 149-157.

List of submissions

[2] Weng Khuen Ho, Arthur Tay, Jiewen Deng, Boon Keng Lok, Thickness uniformity control using Iterative Feedback Tuning, submitted to *IEEE Transactions On Semiconductor Manufacturing, 2003.*